ECS Journal of Solid State Science and Technology, 2020 **9** 016003

Quantum Efficiency Enhancement Depending on the Thickness of p-GaN Spacer Layer in Localized Surface Plasmon-Enhanced Near-Ultraviolet Light-Emitting Diodes by Using Colloidal Silver Nanoparticles

Sang-Hyun Hong,[1] Na-Yeong Kim,[1] Jang-Won Kang,[2] Jae-Joon Kim,[3] Yen-Sook Jung,[4] Dong-Yu Kim,[4] Sang-Youp Yim,[1,z] and Seong-Ju Park[3,z]

[1]*Advanced Photonics Research Institute, Gwangju Institute of Science and Technology, Gwangju 61005, South Korea*
[2]*Department of Emerging Materials Science, Daegu Gyeongbuk Institute of Science and Technology, Daegu 42988, South Korea*
[3]*School of Materials Science and Engineering, Gwangju Institute of Science and Technology, Gwangju 61005, South Korea*
[4]*Department of Nanobio Materials and Electronics, Gwangju Institute of Science and Technology, Gwangju 61005, South Korea*

We demonstrated the dependence on thickness of p-GaN spacer layer in the localized surface plasmons (LSPs)-enhanced near-ultraviolet light-emitting diodes (NUV-LEDs) by pneumatic spray process using colloidal silver (Ag) nanoparticles (NPs). The LSPs-enhanced NUV-LEDs with 10- and 20-nm-thick p-GaN spacer layer showed enhanced internal quantum efficiency (IQE) and reduced effective exciton lifetime by introducing the colloidal Ag NPs. The IQE of LSPs-enhanced NUV-LEDs with 10- and 20-nm-thick p-GaN spacer layer was increased by 18.8% and 24.2%, respectively. These results indicate that the spontaneous emission rate is increased by LSPs-excitons resonant coupling. However, the NUV-LEDs with 40- and 100-nm-thick p-GaN spacer layer showed decreased IQE and extended exciton lifetime due to the evanescent wave property of LSPs field from colloidal Ag NPs.
 [DOI: 10.1149/2.0042001JSS]

Manuscript submitted May 22, 2019; revised manuscript received July 2, 2019. Published August 20, 2019. *This paper is part of the JSS Focus Issue on Recent Advances in Wide Bandgap III-Nitride Devices and Solid State Lighting: A Tribute to Isamu Akasaki.*

Recently, near-ultraviolet light-emitting diodes (NUV-LEDs) are being applied in fields of medical devices, counterfeit detectors, chemical sensors, light source of photometric detectors and pumping source for white LEDs.[1–8] However, the NUV-LEDs in GaN-based LEDs show relatively lower internal quantum efficiency (IQE) compared to blue and green LEDs due to the low indium composition of InGaN quantum well (QW) layers.[8–12] Many research groups have studied to improve the IQE of LEDs by improving GaN-based epilayer quality.[11,13–15] Meanwhile, to overcome the lower IQE problem, the surface plasmon (SP) coupling effect with excitons in multiple quantum wells (MQWs) has been proposed as an efficient IQE improvement by diverse metal structures such as film, grating, protrusion arrays, disks and nanoparticles (NPs). These metal structures are mainly formed through a complex process such as a high vacuum and annealing system (sputter), electron-beam evaporator, lithography, inductively coupled plasma reactive ion etching, thermal furnace and rapid thermal annealing system.[16–22] As an alternative method of metal deposition, the pneumatic spray process is also used for fabricating localized surface plasmons (LSPs)-enhanced LED devices.[23] This LSPs field from metal NPs has evanescent wave property which exponentially decays with the increasing distance between metal NPs and MQWs. Therefore, for the strong LSPs-MQWs resonant coupling, a spacer layer between metal NPs and MQWs plays a prominent role. A thickness of spacer layer for efficient LSPs-MQWs coupling should be thin as tens of nanometers, whereas LSPs-MQWs coupling effect showed weak field intensity in longer thickness of spacer layer more than 40 nm.[16] Several research groups reported the numerical calculation of LSP field variation with various thickness of spacer layer.[24,25] However, there had not been any report of experimental results for practical devices, which require optimized engineering.

In this paper, we investigate the dependence of thickness of p-GaN spacer layer in LSPs-enhanced NUV-LEDs by pneumatic spray process using colloidal silver (Ag) NPs. Temperature dependent (TD) photoluminescence (PL) and time-resolved (TR)-PL measurements are used to observe the LSPs-excitons coupling effect with the various thickness of p-GaN spacer layer. The LSPs-enhanced NUV-LEDs with 10- and 20-nm-thick p-GaN spacer layer showed enhanced IQE and reduced effective exciton lifetime by introducing the colloidal Ag NPs. These results indicate that the spontaneous emission rate is increased by LSPs-excitons resonant coupling. However, the NUV-LEDs with 40- and 100-nm-thick p-GaN spacer layer showed decreased IQE and extended exciton lifetime due to the evanescent wave property of LSPs field from colloidal Ag NPs. The optical output power of LED device is proportional to the external quantum efficiency (EQE) and the EQE is expressed as follows,

$$\eta_{EQE} = \eta_{inj} \times \eta_{rad} \times \eta_{ext}$$

η_{EQE} is the external quantum efficiency, η_{inj} is the injected current, η_{rad} is radiative efficiency and η_{ext} is extraction efficiency. $\eta_{inj} \times \eta_{rad}$ is referred to as IQE. It can be estimated that the change of IQE in MQWs would affect LED device performance. These practical results will help further studies of structure design in LSP-enhanced NUV-LEDs.

Experimental

Fabrication of LSPs-enhanced NUV-LEDs.—The NUV-LEDs were grown on a c-plane sapphire (0001) substrate by metal organic chemical vapor deposition (MOCVD). A 25-nm-thick GaN nucleation layer was grown at 550°C. Subsequently, a 2-μm-thick un-doped GaN layer and a 2-μm-thick Si-doped n-GaN layer were grown at 1020°C. Then, five pairs MQWs consisting of 3-nm-thick un-doped InGaN wells and 12-nm-thick Si-doped GaN barriers were grown at 770°C. And then, a p-GaN spacer layer with the thickness of 10, 20, 40, and 100 nm was grown on the MQWs at 950°C, respectively. The reference sample was grown 200-nm-thick p-GaN layer on MQWs structure at 950°C. The colloidal Ag NPs were deposited on each p-GaN spacer layer by pneumatic spray process. After the spray process, a 30-nm-thick low temperature p-GaN (750°C) as a capping layer and a p-GaN layer (950°C) were regrown on the sprayed colloidal Ag NPs, which were embedded in the 200-nm-thick p-GaN layer.

Preparation of solution-based colloidal Ag NPs.—The solution-based Ag NPs fabricated by using chemical solution method was

[z]E-mail: syim@gist.ac.kr; sjpark@gist.ac.kr

commercially available and we purchased the pre-synthesized 10-nm-sized Ag NPs solution from SIGMA ALDRICH, USA. The concentration and average diameter of colloidal Ag NPs in solution are 0.02 mg/mL and 10 nm in aqueous buffer (deionize water) with sodium citrate stabilizer, respectively. And, the density of colloidal Ag NPs in solution is 0.997 g/mL at 25°C.

Preparation of deposition of colloidal Ag NPs by pneumatic spray process.—We employed a pneumatic spray nozzle (two-fluid type) which uses the pressurized N_2 gas to break up the liquid bulk (colloidal Ag NPs in aqueous solution). The pre-synthesized colloidal Ag NPs solution (1 mL) consisting of Ag NPs, stabilizer (sodium citrate), and aqueous buffer (deionize water) was injected into fluid cup and sprayed at a N_2 gas pressure of 0.3 MPa using a flow rate of 0.15 mL/min. The size of spray nozzle (IWATA air-brush HP-SBP, Japan) is 0.2 mm. The distance between the nozzle of the spray apparatus and the sample was maintained at 180 mm. After the spray process, we rinsed the samples in running isopropyl alcohol for 30 sec to remove the residual stabilizer which prevents the agglomeration of deposited Ag NPs during the evaporation of the solvent.

Characterization of the LSPs-enhanced NUV-LEDs with various thickness of p-GaN spacer layer.—TD-PL spectra of the LSPs-enhanced NUV-LEDs with various thickness of p-GaN spacer layer and reference sample were observed using a UV-Vis spectrometer (USB4000, Ocean Optics, USA) with a 325 nm He-Cd laser (KIMMON KOHA, Japan) as the excitation source. Cryogenic system is used for TD-PL measurement (CCS-150, JANIS, USA). The light source of TR-PL measurement is a 710 nm-wavelength of Ti:sapphire laser (MaiTai, Spectra Physics, USA) with 100 fs pulse width and repetition rate of 80 MHz, which is additionally reduced to 4.44 MHz by pulse picker to obtain a temporal widow as 200 ns. The frequency of laser is doubled to 355 nm by β-BaB_2O_4 crystal. To observe TR-PL decay graph, a 30 cm monochromator dispersed the collected PL and a streak scope (C10627, Hamamatsu K. K., Japan) detected it. The absorbance spectra were measured by using a UV-Vis spectrophotometer (Agilent 8453, Agilent Technologies, USA). The structural analysis was observed by using a field emission scanning electron spectroscopy (FE-SEM) (JSM-7500F, JEOL, USA).

Results and Discussion

Figures 1a–1c show a fabrication process of the LSPs-enhanced NUV-LEDs with the various thickness of p-GaN spacer layer. Figure 1d shows the schematic diagram of LED A, B, C, D and reference LED as a function of p-GaN spacer layer thickness, respectively. The LED A, B, C and D have 10-, 20-, 40- and 100-nm-thick p-GaN spacer layer with colloidal Ag NPs and metal NPs are embedded in 200-nm-thick p-GaN layer as shown in Figs. 1b and 1c. The reference LED is conventional LED structure (200-nm-thick p-GaN layer) without colloidal Ag NPs.

Figure 2a shows the schematic diagram of pneumatic spray process. We used a pneumatic spray nozzle which the pressurized N_2 gas to break up the solution-based colloidal Ag NPs as explained in detail above. A high-velocity gas from pneumatic spray nozzle collides with the liquid bulk, leading to disintegration of the liquid into small droplets by high frictional forces between gas and liquid surface. Figure 2b shows the FE-SEM image of colloidal Ag NPs on the p-GaN

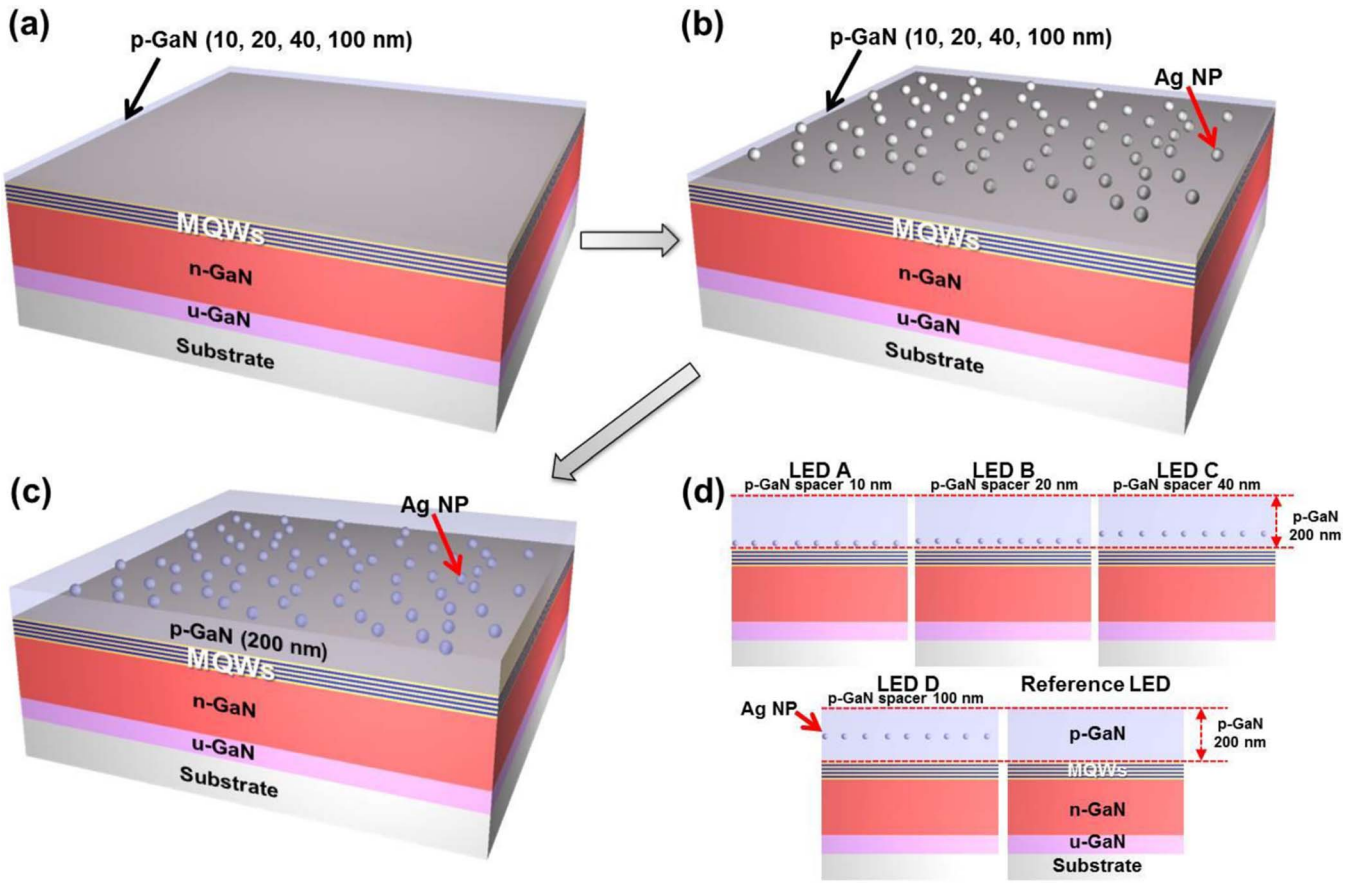

Figure 1. Fabrication process of the LSPs-enhanced NUV-LEDs with the various thickness of p-GaN spacer layer. (a) 10-, 20-, 40-, and 100 nm-thick p-GaN spacer layer on the InGaN/GaN NUV-MQWs. (b) Deposited colloidal Ag NPs by spray process on the p-GaN spacer layer. (c) Regrown p-GaN layer on the colloidal Ag NPs, which were embedded in the p-GaN layer (totally 200 nm). (d) Schematic diagram of cross-sectional LED A, B, C, D and reference LED as a function of p-GaN spacer layer thickness, respectively.

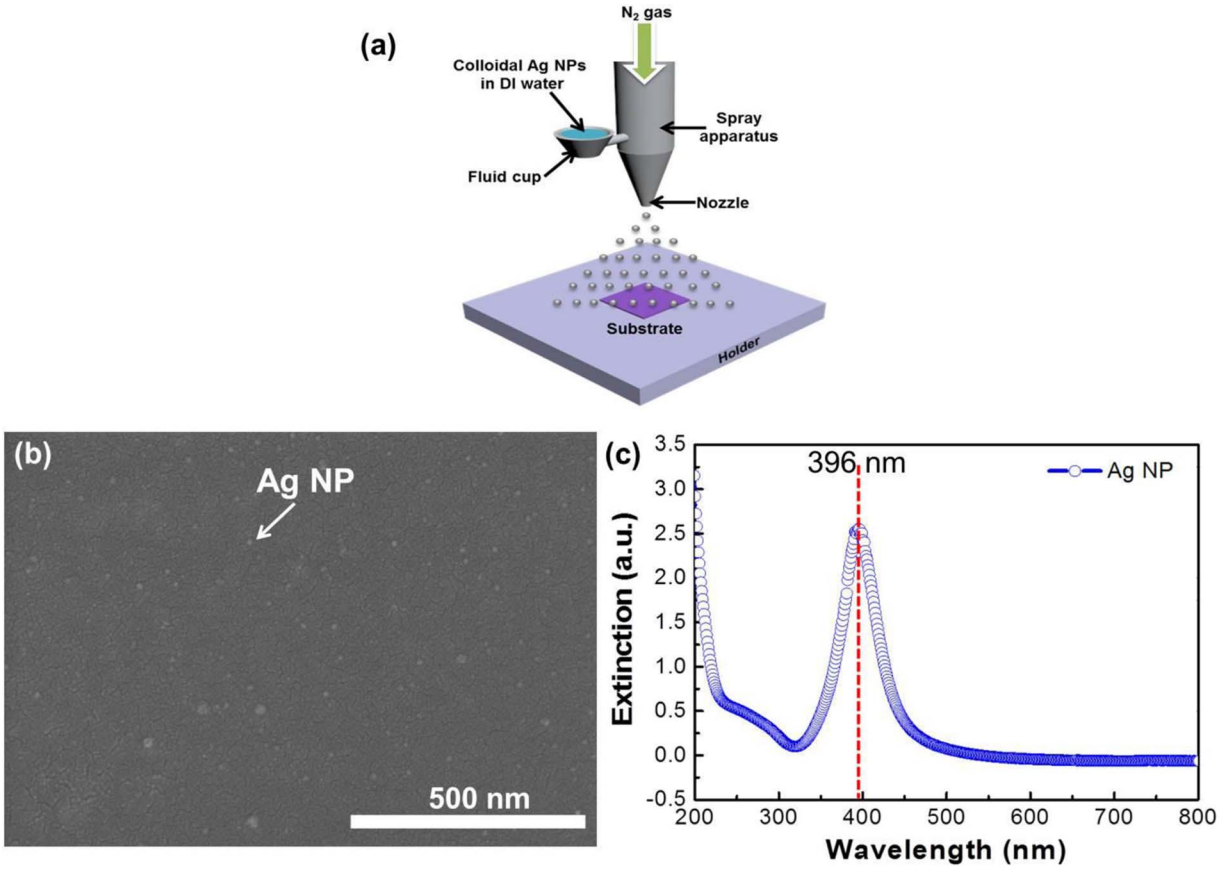

Figure 2. (a) Schematic diagram of pneumatic spray process. (b) FE-SEM image of deposited colloidal Ag NPs on the p-GaN spacer layer by spray process. (c) Absorbance spectrum of colloidal Ag NPs as a function of wavelength.

spacer layer after the spray process. The diameter and density of colloidal Ag NPs are in the range of 5–19 nm and 2×10^{10} cm^{-1}, respectively. The surface coverage of colloidal Ag NPs is $\sim 6.32\%$ and it is optimized condition for the regrowth of p-GaN layer and leakage currents compared to the previous results.[23,26,27] Figure 2c shows the absorbance spectrum of colloidal Ag NPs embedded in p-GaN (180-nm-thick p-GaN/colloidal Ag NPs/20-nm-thick p-GaN on sapphire) and the main peak of absorbance is 396 nm. This SP characteristic peak is close to the 398 nm of emission wavelength of the NUV-LEDs. Therefore, a strong LSPs-excitons resonant coupling is expected in LSP-enhanced NUV-LEDs.

Figures 3a and 3b show the temperature-dependent photoluminescence (PL) spectra of LED A, B, C, D and reference LED at 300 K and 10 K, respectively. The IQE of each LED samples was calculated by comparison of the integrated PL intensities, supposing that the IQE is 100% at 10 K.[16] In Figure 3a shows PL peaks (398 nm) of LED A and B were slightly blue-shifted from reference LED (399 nm). Note that the difference of main peaks is not significant, but the shape of spectra is slightly blue-shifted due to the SP characteristic peak of 396 nm. The resonant coupling by local electric fields in metal NPs influence on the wavelength of LSP-enhanced MQWs. The IQEs of LED samples are calculated to be 52.6% (LED A), 55.1% (LED B), 18.2% (LED C) and 17.9% (LED D), respectively, and that of reference LED is 44.3%. The IQE enhancement ratios of LED samples had increased by 18.8% (LED A) and 24.2% (LED B), whereas the those of LED C and D are decreased by 58.9% and 59.6% as increasing the thickness of p-GaN spacer layer above 40 nm as shown in Fig. 3c. For the LED A and B, LSPs-excitons resonant coupling effect has influence to enhanced IQE compared to LED C and D due to the relatively thinner p-GaN spacer layer. And, the IQE enhancement ratios of LED C and D indicate that LSPs-excitons coupling process shows weak behavior in 40- and 100-nm-thick p-GaN spacer layer due to the evanescent wave property of LSP field. This local electric field is exponentially decayed as increasing the distance between colloidal Ag NPs and MQWs. In addition, the intensity of laser light reduced due to absorption, scattering and reflection by colloidal Ag NPs embedded in p-GaN layer, turning the incident laser light toward the top side of NUV-LED structure. Absorption, scattering, and reflection effects are expected to occur once again in the process of radiative recombination of excitons in MQWs. At the same time, absorption of NUV wavelength is also expected to occur in the low temperature regrown p-GaN capping layer due to the crystal quality of low temperature (750°C) p-GaN layer is lower than that of high temperature (950°C) p-GaN layer. However, LSPs-excitons coupling effect overcomes these problems for LED A and B due to the 10- and 20-nm-thick p-GaN spacer layer compared to LED C and D. This is because a thin spacer layer of less than 20-nm-thick are easily to grow into a 3D-like structure during p-GaN regrowth process by MOCVD. This inclement crystal quality of spacer layer is expected to act as an optical loss of exciton in MQWs.

Figure 4 show the TR-PL spectra of the NUV-LEDs with colloidal Ag NPs as a function of p-GaN spacer layer thickness. The TR-PL measurements were conducted at 10 K to exclude non-radiative recombination process from excitons that contends with the LSPs resonant coupling. The radiative decay of exciton can be shown as following double exponential decay calculation.

$$I_{(t)} = A_1 e^{-t/\tau_1} + A_1 e^{-t/\tau_2},$$

where t is the time, A_1 and A_2 are the normalization constant and τ_1 and τ_2 are decay lifetime. To calculate the LSPs-excitons resonant coupling between colloidal Ag NPs and MQWs, the fast and slow decay regions of each decay curve are fitted by a double exponential

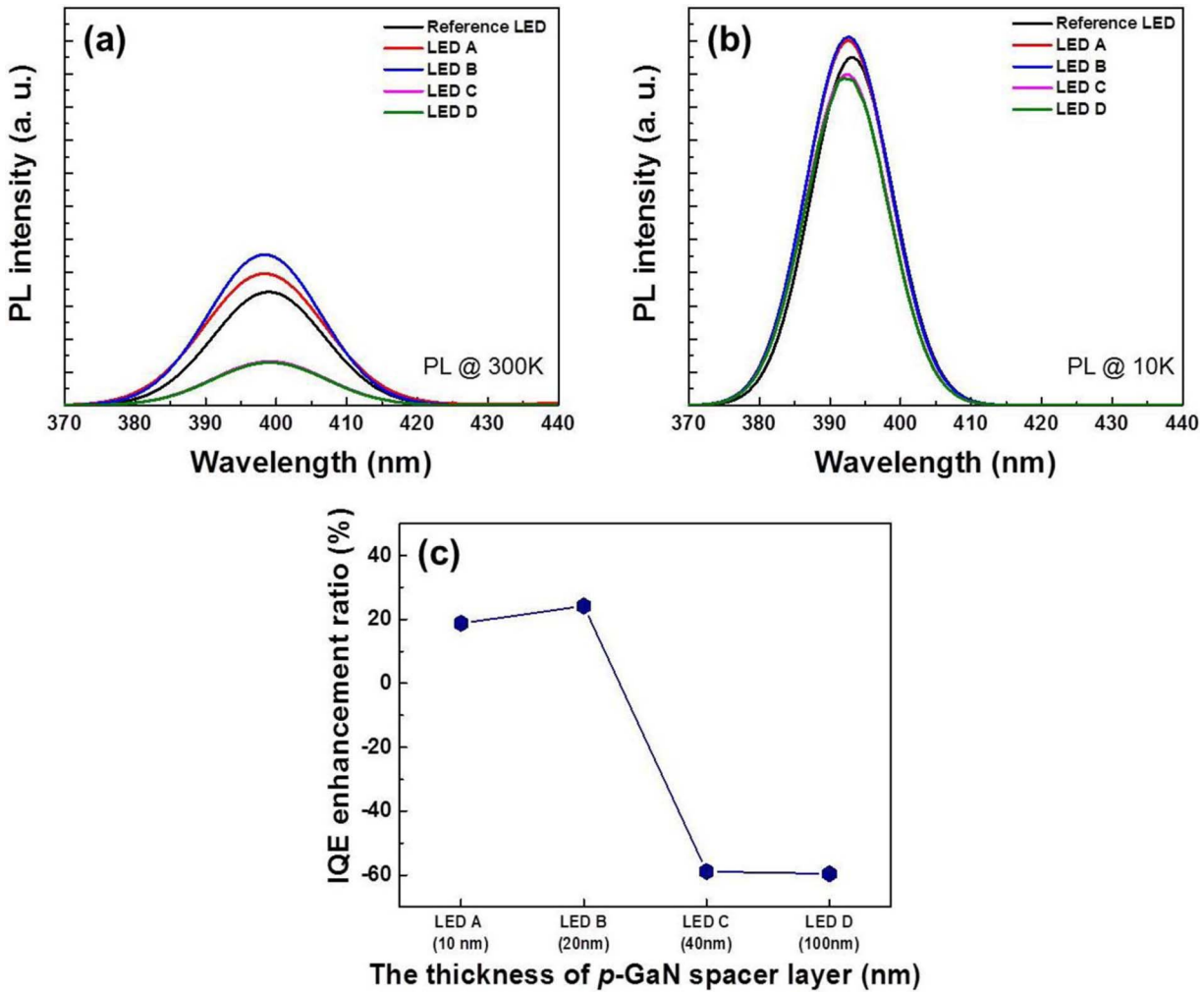

Figure 3. (a) PL spectra of LSPs-enhanced NUV-LEDs with various thickness of p-GaN spacer layer and reference LED (without colloidal Ag NPs) (a) at 300 K and (b) 10 K. (c) IQE enhancement ratios of LSPs-enhanced NUV-LEDs with various thickness of p-GaN spacer layer compared to reference NUV-LED.

decay calculation. The fast decay region (τ_1) indicates the fast exciton recombination process corresponding to the effective exciton lifetime, whereas the slow decay region (τ_2) indicates the localized carrier recombination process.[28–30] The τ_1 values of NUV-LEDs with colloidal Ag NPs are 0.628 ns (LED A), 0.592 ns (LED B), 0.672 ns (LED C), and 0.728 ns (LED D), respectively, and that of reference LED (without colloidal Ag NPs) is 0.656 ns as shown in Fig. 4. The decreased decay time in LED A and B compared to reference LED indicate that the spontaneous emission rate can be increased by efficient LSPs-excitons coupling via a new SP recombination channel.[28–31] Further, the τ_1 of LED C and D are longer decay time than that of reference LED due to weak LSP field in the range of relatively thicker thickness of p-GaN spacer layer. In Figure 4, the effective exciton lifetime of LED C and D compared to reference LED represent decreased spontaneous emission rate alike as IQE enhancement ratio from TD-PL results shown in Fig. 3c. In these results, the difference in the decay lifetimes between reference LED and LED A is −0.028 ns, while that between reference LED and LED C is +0.016 ns. In spite of that, the IQE differences in LED C is larger than LED A compared to reference LED. The lifetime of excitons affects to the spontaneous emission from MQWs. This result comes from difference in the measurement methods of TD-PL and TR-PL. In case of TD-PL, incident laser light irradiated toward the top side of LED structure, whereas, in case of TR-PL, incident laser light irradiated toward the bottom side of LED structure. Thereby, it is estimated that the effect on absorption on the low temperature p-GaN layer has been relatively small for the results of TR-PL measurements. In general, the local electric fields from metal NPs has a characteristics of evanescent wave, but in Figures 3 and 4, the LED B (20-nm-thick spacer layer) shows higher performance than the LED A (10-nm-thick spacer layer). This is because a thin spacer layer than 20 nm have an adverse effect on the regrowth layer. Therefore, the optimized distance between metal NPs and MQWs is 20 nm due to the characteristics of SP and growth technique by MOCVD in GaN-based LEDs.

Conclusions

We demonstrated the LSPs-enhanced NUV-LEDs with diverse thickness of p-GaN spacer layer. The solution-based colloidal Ag NPs for LSP coupling effect are deposited by pneumatic spray process. The IQE of LSPs-enhanced NUV-LEDs with 20-nm-thick p-GaN spacer layer is increased by 24.2% than that of NUV-LEDs without colloidal Ag NPs. In GaN-based LEDs, the optimized distance between metal NPs and MQWs is 20 nm due to the characteristics of SP and growth technique. The TR-PL measurements indicate the effective exciton lifetime is decreased in LSPs-enhanced NUV-LEDs with 10-nm ($\tau_1 = 0.628$ ns) and 20-nm ($\tau_1 = 0.592$ ns) thick p-GaN spacer layer compared with reference LED ($\tau_1 = 0.656$ ns). In general, metal NPs are loss channels due to absorption, scattering, and reflection of light emission, however, the improved spontaneous emission rate by LSPs coupling effect overcomes loss rate when the distance between metal NPs and MQWs is 20 nm and

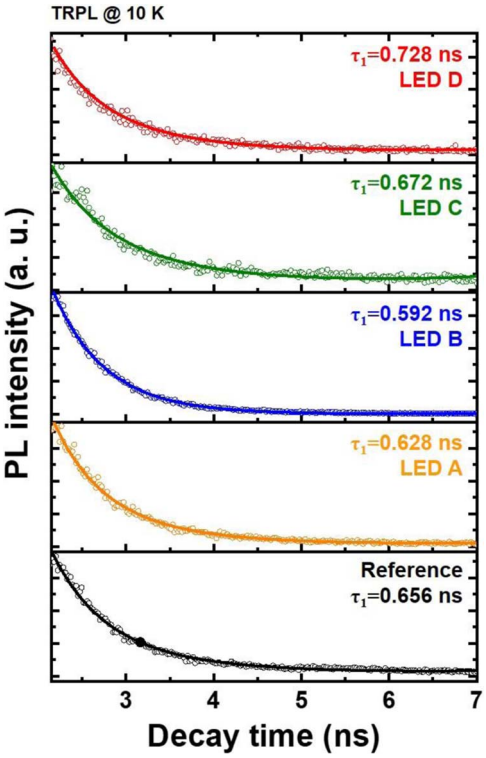

Figure 4. TR-PL spectra of the NUV-LEDs with and without colloidal Ag NPs at LED A, LED B, LED C and LED D, compared with reference LED.

below. These optical properties lead us to the conclusion that the optimized thickness of spacer layer is 20 nm in NUV-LEDs for efficient LSPs-excitons coupling between colloidal Ag NPs and MQWs. In addition, we expected to effective design of LED structure with LSPs coupling.

Acknowledgments

This research was supported by the GIST Research Institute (GRI) grant funded by the GIST.

ORCID

Sang-Youp Yim https://orcid.org/0000-0001-5503-6957
Seong-Ju Park https://orcid.org/0000-0002-8971-4290

References

1. P. Waltereit, O. Brandt, A. Trampert, H. T. Grahn, J. Menniger, M. Ramsteiner, M. Reiche, and K. H. Ploog, *Nature*, **406**, 865 (2000).
2. T. Wang, Y. H. Liu, Y. B. Lee, J. P. Ao, J. Bai, and S. Sakai, *Appl. Phys. Lett.*, **81**, 2508 (2002).
3. A. Knauer, H. Wenzel, T. Kolbe, S. Einfeldt, M. Weyers, M. Kneissl, and G. Tränkle, *Appl. Phys. Lett.*, **92**, 191912 (2008).
4. C. H. Huang, D. Y. Wang, Y. C. Chiu, Y. T. Yeh, and T. M. Chen, *RSC Adv.*, **2**, 9130 (2012).
5. L. Wang, X. Wang, T. Takeda, N. Hirosaki, Y. T. Tsai, R. S. Liu, and R. J. Xie, *Chem. Mater.*, **27**, 8457 (2015).
6. K. Song, M. Mohseni, and F. Taghipour, *Water Res.*, **94**, 341 (2016).
7. H. Jeong, S. Y. Jeong, D. J. Park, H. J. Jeong, S. Jeong, J. T. Han, H. J. Jeong, S. Yang, H. Y. Kim, K. J. Baeg, S. J. Park, Y. H. Ahn, E. K. Suh, G. W. Lee, Y. H. Lee, and M. S. Jeong, *Sci. Rep.*, **5**, 7778 (2015).
8. S. Zhao, M. Djavid, and Z. Mi, *Nano Lett.*, **15**, 7006 (2015).
9. T. Nishida, H. Saito, and N. Kobayashi, *Appl. Phys. Lett.*, **79**, 711 (2001).
10. M. Kunzer, U. Kaufmann, K. Köhler, C. C. Leancu, S. Liu, and J. Wagner, *Phys. Stat. Sol. (c)*, **4**, 2822 (2007).
11. S. Watanabe, N. Yamada, Y. Ueki, C. Sasaki, Y. Yamada, T. Taguchi, K. Tadatomo, H. Okagawa, and H. Kudo, *Appl. Phys. Lett.*, **83**, 4906 (2003).
12. K. Y. Woo, K. H. Kim, and T. G. Kim, *IEEE Photon. Technol. Lett.*, **28**, 67 (2016).
13. C. H. Wang, C. C. Ke, C. H. Chiu, J. C. Li, H. C. Kuo, T. C. Lu, and S. C. Wang, *J. Cryst. Growth*, **315**, 242 (2011).
14. M. Kunzer, U. Kaufmann, K. Kohler, C. C. Leancu, S. Liu, and J. Wagner, *Phys. Stat. Sol. (c)*, **4**, 2822 (2007).
15. S. C. Huang, K. C. Shen, D. S. Wuu, P. M. Tu, H. C. Kuo, C. C. Tu, and R. H. Horng, *J. Appl. Phys.*, **110**, 123102 (2001).
16. K. Okamoto, I. Niki, A. Shvartser, Y. Narukawa, T. Mukai T, and A. Scherer, *Nat. Mater.*, **3**, 601 (2004).
17. M. K. Kwon, J. Y. Kim, B. H. Kim, I. K. Park, C. Y. Cho, C. C. Byeon, and S. J. Park, *Adv. Mater.*, **20**, 1253 (2008).
18. D. M. Yeh, C. F. Huang, C. Y. Chen, Y. C. Lu, and C. C. Yang, *Appl. Phys. Lett.*, **91**, 171103 (2007).
19. H. S. Chen, C. F. Chen, Y. Kuo, W. H. Chou, C. H. Shen, Y. L. Jung, Y. W. Kiang, and C. C. Yang, *Appl. Phys. Lett.*, **102**, 041108 (2013).
20. C. Y. Cho, J. J. Kim, S. J. Lee, S. H. Hong, K. J. Lee, S. Y. Yim, and S. J. Park, *Appl. Phys. Express*, **5**, 122103 (2012).
21. C. Y. Cho, S. J. Lee, J. H. Song, S. H. Hong, S. M. Lee, Y. H. Cho, and S. J. Park, *Appl. Phys. Lett.*, **98**, 051106 (2011).
22. Y. Ou, D. Iida, J. Liu, K. Wu, K. Ohkawa, A. Boisen, P. M. Petersen, and H. Ou, *Nanophotonics*, **7**(1), 317 (2018).
23. S. H. Hong, J. J. Kim, J. W. Kang, Y. S. Jung, D. Y. Kim, S. Y. Yim, and S. J. Park, *Nanotechnology*, **26**, 385204 (2015).
24. J. B. Khurgin, G. Sun, and R. A. Soref, *Appl. Phys. Lett.*, **93**, 021120 (2008).
25. L. W. Jang, D. W. Jeon, T. Sahoo, D. S. Jo, J. W. Ju, S. Lee, J. H. Baek, J. K. Yang, J. H. Song, A. T. Polyakov, and I. H. Lee, *Opt. Express*, **20**, 2116 (2012).
26. S. H. Hong, C. Y. Cho, S. J. Lee, S. Y. Yim, W. Lim, S. T. Kim, and S. J. Park, *Opt. Express*, **21**, 3138 (2013).
27. C. Y. Cho, M. K. Kwon, S. J. Lee, S. H. Han, J. W. Kang, S. E. Kang, D. Y. Lee, and S. J. Park, *Nanotechnology*, **21**, 205201 (2010).
28. C. K. Choi, Y. H. Kwon, B. D. Little, G. H. Gainer, J. J. Song, Y. C. Chang, S. Keller, U. K. Mishra, and S. P. DenBaars, *Phys. Rev. B*, **64**, 245339 (2001).
29. Q. J. Ren, S. Filippov, S. L. Chen, M. Devika, N. K. Reddy, C. W. Tu, W. M. Chen, and I. A. Buyanova, *Nanotechnology*, **23**, 425201 (2012).
30. E. Cao, W. Lin, M. Sun, W. Liang, and Y. Song, *Nanophotonics*, **7**(1), 145 (2018).
31. S. W. Feng, Y. C. Cheng, Y. Y. Chung, C. C. Yang, M. H. Mao, Y. S. Lin, K. J. Ma, and J. I. Chyi, *Appl. Phys. Lett.*, **80**, 4375 (2002).